

## Supporting Information

### Single Crystalline $\text{Cu}_2\text{ZnSnS}_4$ Nanosheet Arrays for Efficient Photochemical Hydrogen Generation

Bo-Jun Li,<sup>†</sup> Peng-Fei Yin,<sup>†</sup> Yu-Zhu Zhou, Zhi-Ming Gao, Tao Ling, \*Xi-Wen Du\*

#### Part 1. Characterization of CuCl film

CuCl film was grown on a FTO substrate by physical vapor deposition. Figure S1a shows that the film consists of a lot of large grains. The XRD pattern (Figure S1b) confirms that the phase of the raw material is unchanged after high temperature processing.

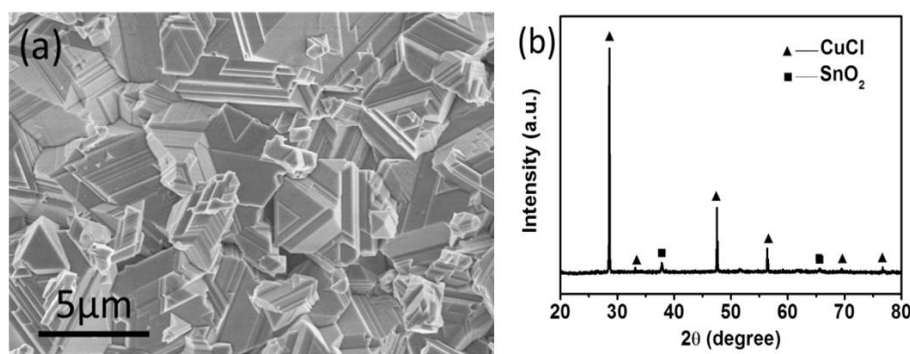
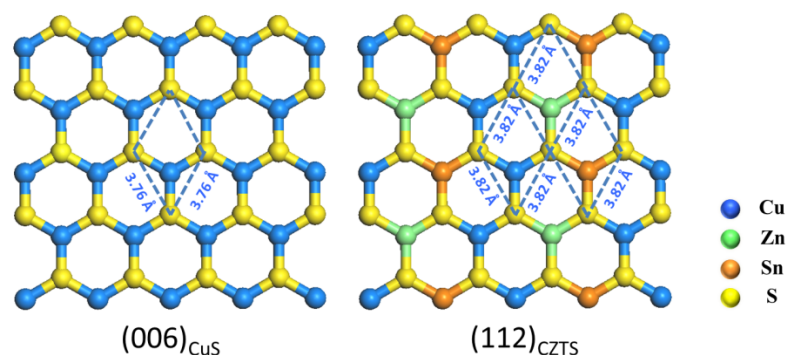


**Figure S1.** Characterization of CuCl film. (a) and (b) are top-view SEM image and XRD spectrum of CuCl film on a conductive glass substrate, respectively.

#### Part 2. The structure analysis of CuS and CZTS

The lattices of CuS and CZTS matched very well, with the discrepancies between {110} CuS ( $d=1.89\text{\AA}$ ) and {220} CZTS ( $d=1.91\text{\AA}$ ) less than 2%. The S atomic arrangements in (006)CuS and (112) CZTS are similar. As shown in Scheme S1, The S atomic arrangement in (006)CuS is comprised of parallelograms with  $3.76\text{\AA}$  in side length and  $60^\circ$  in angle. And S atoms in (112) CZTS are structurally arranged in three types of quadrangles with the same side lengths and angles. The lattice match and similarity of S atomic arrangements facilitate the epitaxial

growth of CZTS nanosheet (NS) with (112) facets preferentially exposed on the (006) facets of CuS NS via a cation exchange process. The conversion mechanism can be expressed as the following:



**Scheme S1.** S atomic arrangements in (006) CuS and (112) CZTS.

### Part3. Synthesis and Characterization of CuSNSAs

As shown in Scheme 2a, Cu atoms in the parent CuCl film react with the sulfur vapor to form crystal nuclei. It is believed that the CuS crystal nuclei preferentially grow on the  $(10\bar{1}0)$  and  $(11\bar{2}0)$  planes and more slowly on the (0001) plane. Thus, NS morphology formed with exposed (0001) plane with low surface energy.<sup>[S1]</sup> Figure S2a is an enlarged SEM image of CuS NS, showing the thickness of CuS NS is approximately 30 nm. Figure S2b is a EDS spectrum of CuS NSs, which indicates an Cu/S atomic ratio of 48:52.

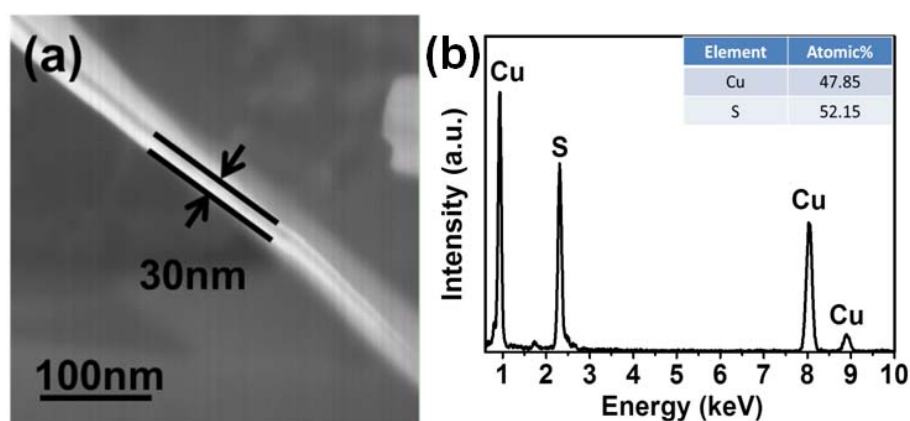


**Figure S2.** (a) SEM image of a CuS NS, showing the thickness of CuS NS is approximately

30 nm, (b) EDS spectrum obtained from CuS NSs.

#### Part 4.Characterization of CZTS NSs

The spatial distribution of Cu, Zn, Sn, and S elements is obtained from the STEM-EDS elemental mapping. Figure 4c shows the darkfield image of a single CZTS NS. And Figure S3b-3e are the elemental maps of S, Cu, Zn and Sn, respectively, showing uniform distribution of all compositional elements in the NS. The quantitative analysis of the EDS data (Figure S3f) suggests the composition of the NS is close to the stoichiometry of  $\text{Cu}_2\text{ZnSnS}_4$  (Cu/Zn/Sn/S  $\sim$  2.0/1.0/1.0/3.9).

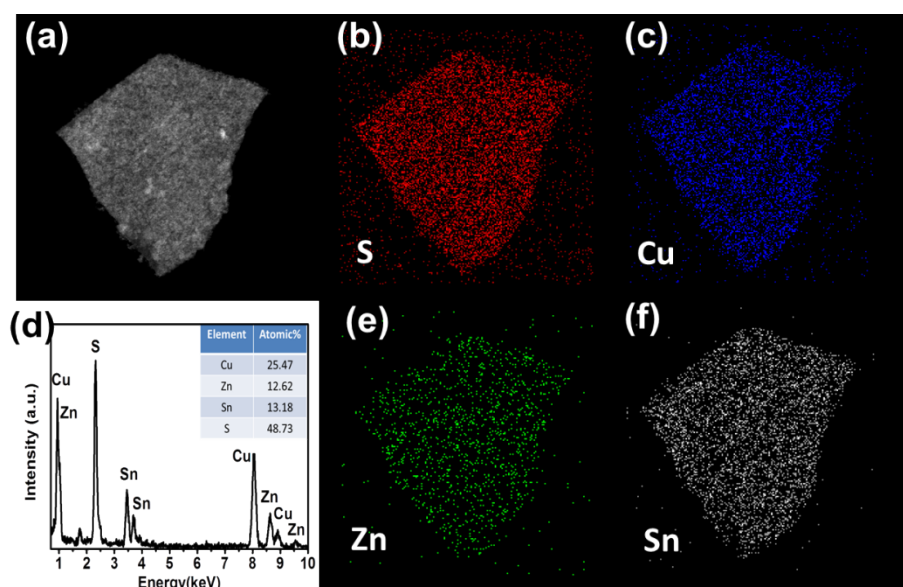


**Figure S3.** STEM-EDS elemental map and EDS of a single CZTS NS.

Raman spectrum was further used to verify the structure information of CZTS NSs. The intense peak at  $332\text{ cm}^{-1}$  (Figure S4) is the characteristic peak of CZTS and close to the reported values.<sup>[S2-S4]</sup> No other characteristic peaks of impurities were observed, such as  $\text{Cu}_2\text{xS}$  ( $475\text{ cm}^{-1}$ ), ZnS ( $351\text{ cm}^{-1}$  and  $274\text{ cm}^{-1}$ ),  $\text{Cu}_3\text{SnS}_4$  ( $318, 348$  and  $295\text{ cm}^{-1}$ ).<sup>[S5]</sup> This result excluded the presence of other binary or ternary impurity phases, and confirmed the composition of nanosheet arrays by only CZTS.

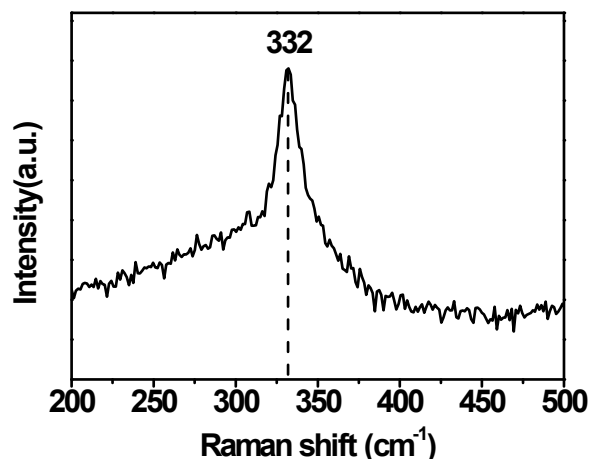


**Figure S4.** Raman spectrum of the as-synthesized CZTS NSs.

The direct optical band gap, 1.43 eV, of CZTS NSs was calculated from the UV–vis spectrum (Figure S5) by the extrapolation of the linear region of a plot of  $(\alpha h\nu)^2$  versus energy, where  $\alpha$  represents the absorption coefficient and  $h\nu$  is the photon energy.

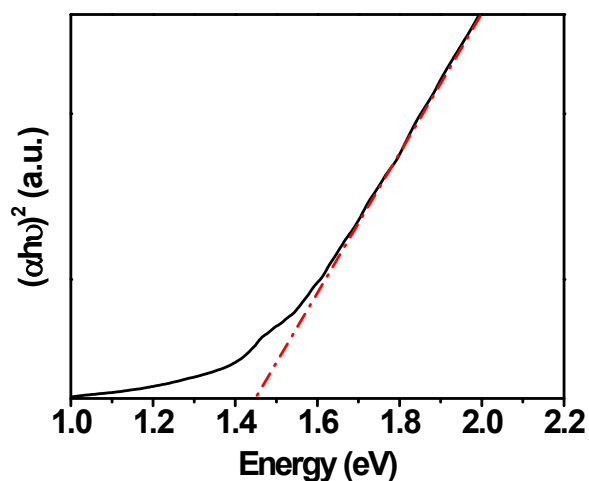


**Figure S5.** The plots of  $(\alpha h\nu)^2$  versus  $h\nu$  for the CZTS NSs.

Moreover, the specific surface area of CZTS NSs were estimated based on atomic absorption analysis. We dissolved 1.88 cm<sup>2</sup> CZTS NSAs into concentrated nitric acid, and the weight of Cu element is measured as 0.23 mg. Then, the weight of CZTS NSAs on per cm<sup>2</sup>FTO substrate was calculated as 42 mg. Thus, the surface area of CZTS NSs on per cm<sup>2</sup>FTO substrate was calculated using the following equation,

$$S_{CZTS} = \frac{m_{CZTS}}{\rho_{CZTS} d_{CZTS}} \times 2 \quad (S2)$$

where  $m_{CZTS}$  is the weight of CZTS NSAs on per  $\text{cm}^2$  FTO substrate,  $\rho_{CZTS}$  is the density of CZTS with the value of  $4.56 \text{ g/cm}^3$ , and  $d_{CZTS}$  is thickness of CZTS NSs determined to be about  $35 \text{ nm}$  by AFM characterization shown in Figure 2c. Hence,  $S_{CZTS}$  is calculated as  $22.6 \text{ m}^2/\text{g}$ .

### Part 5.Characterization of CZTS film

The CZTS film was synthesized according to the method describing in the experimental section. The synthesized CZTS film was characterized by SEM and XRD. As seen in Figure S6a, the surface of as-synthesized film is flat and smooth. The side-view SEM image (Figure S6b) shows that the thickness of the film was about  $1 \mu\text{m}$ . The XRD pattern (Figure S6c) exhibits diffraction peaks corresponding to the CZTS, in addition to diffraction peaks of  $\text{SnO}_2$ , which ascribing to the FTO substrate.

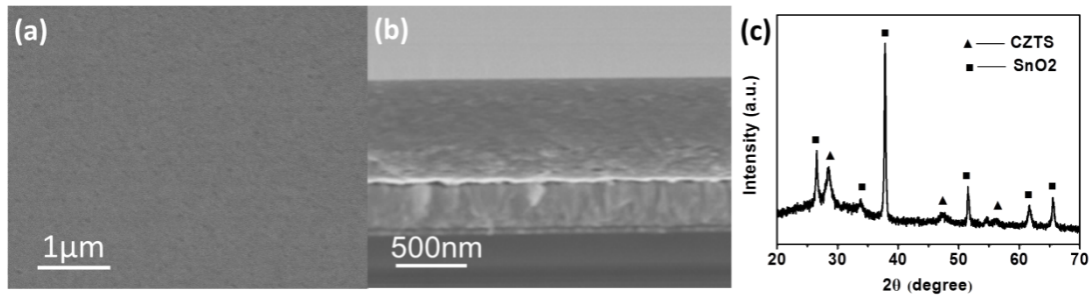


**Figure S6.** Characterization of CZTS film. (a) and (b) are top-view and side-view SEM images of CZTS film on a conductive glass substrate, respectively. (c) XRD spectrum of the CZTS film.

### Part 6. Mott-Schottky analysis

The acceptor density,  $N_A$ , was calculated from the slopes of the Mott-Schottky plots (Figure S7) by the following equation,

$$\frac{dC^{-2}}{dV} = \frac{-2}{q\epsilon_0\epsilon_r N_A A^2} \quad (S3)$$

where  $A$  is the surface area of the measured sample,  $\epsilon_r$  is the dielectric constant of CZTS with the value of 7.0. The acceptor concentration  $N_A$  is obtained as  $3.68 \times 10^{20} \text{ cm}^{-3}$  from the provided Mott-Schottky plot.

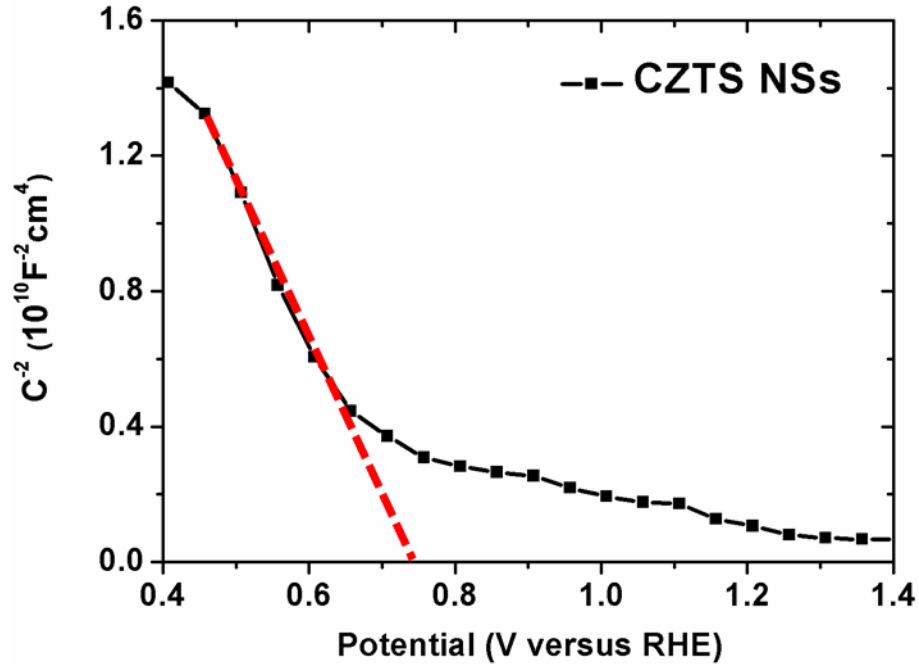


**Figure S7.** Mott-Schottky plot of CZTS, and the flat-band potential is obtained from the intercept of the extrapolated line.

**Part 7. The experimental reflectance spectra of the CZTS film and NSAs structure**

Figure S8 shows the reflectance spectra of CZTS film and NSAs. As seen, the reflectance intensity of CZTS film is higher than that of NSAs during the whole detected wavelength range.

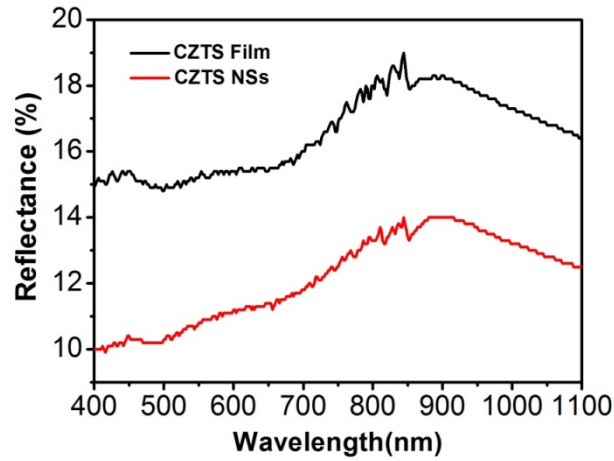


**Figure S8.** The reflectance spectra of CZTS film and NSAs.

### Part 8. FDTD Simulation

All the FDTD simulations were carried out using a commercial software, Lumerical. Total simulation time is 1000 fs, and time step for every calculation is 0.02fs. The 2-D models used in simulation are shown in **Figure S9**, and the boundary conditions in  $x$  and  $y$  directions are periodic and perfectly matched layer (PML), respectively. The electric field distribution is simulated by calculating the electric field intensity per unit volume. To simulate the absorption spectrum, several 2-D power monitors are located at the boundaries to measure the amount of power flowing into and out of the samples. The total absorption corresponds to the difference between these values. The simulation of absorption profile is based on the formula:  $P_{abs} = -P_{abs}|E|^2 \text{imag}(\epsilon)$ , where  $P_{abs}$  represents the power absorption per unit volume,  $\omega$  is the angular frequency,  $|E|$  is the electric field intensity and  $\text{imag}(\epsilon)$  is the imaginary part of the permittivity.

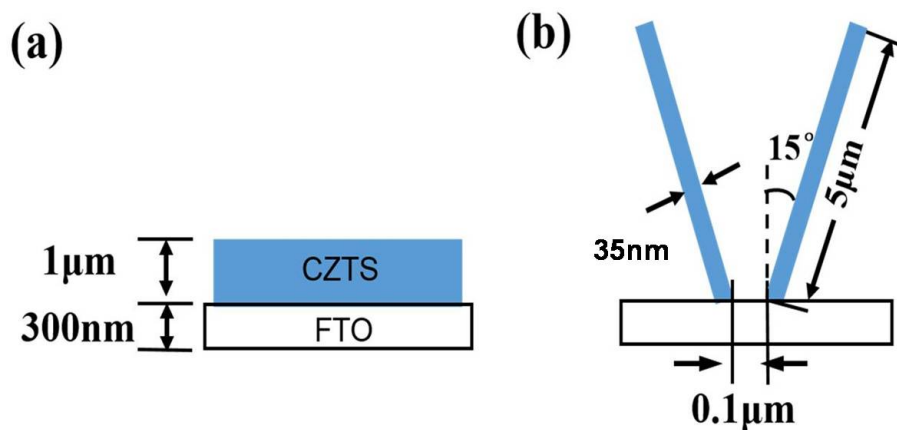


**Figure S9.** Simulated geometrical models of (a) CZTS film and (b) CZTS NSAs arrays samples.

### Supplementary References

[S1] K. J. Wang, G. D. Li, J. X. Li, Q. Wang, J. S. Chen, *Cryst. Growth Des.* **2007**, *7*, 2265-2267.

[S2] Z. H. Su, C. Yan, D. Tang, K. W. Sun, Z. L. Han, F. Y. Liu, Y. Q. Lai, J. Li, Y. X. Liu, *Crystengcomm* **2012**, *14*, 782-785.

[S3] S. Wozny, K. Wang, W. L. Zhou, *J. Mater. Chem. A* **2013**, *1*, 15517-15523.

[S4] X. Xin, M. He, W. Han, J. Jung, Z. Lin, *Angew. Chem. Int. Ed.* **2011**, *50*, 11739-42.

[S5] W. H. Zhou, Y. L. Zhou, J. Feng, J. W. Zhang, S. X. Wu, X. C. Guo, X. Cao, *Chem. Phys. Lett.* **2012**, *546*, 115-119.